

Argonne National Laboratory

A PROTOTYPE ANALOG REACTIVITY METER FOR EBR-II

by

J. R. Karvinen, R. W. Hyndman,
R. A. Call, and C. C. Price

The facilities of Argonne National Laboratory are owned by the United States Government. Under the terms of a contract (W-31-109-Eng-38) between the U. S. Atomic Energy Commission, Argonne Universities Association and The University of Chicago, the University employs the staff and operates the Laboratory in accordance with policies and programs formulated, approved and reviewed by the Association.

MEMBERS OF ARGONNE UNIVERSITIES ASSOCIATION

The University of Arizona
Carnegie-Mellon University
Case Western Reserve University
The University of Chicago
University of Cincinnati
Illinois Institute of Technology
University of Illinois
Indiana University
Iowa State University
The University of Iowa

Kansas State University
The University of Kansas
Loyola University
Marquette University
Michigan State University
The University of Michigan
University of Minnesota
University of Missouri
Northwestern University
University of Notre Dame

The Ohio State University
Ohio University
The Pennsylvania State University
Purdue University
Saint Louis University
Southern Illinois University
The University of Texas at Austin
Washington University
Wayne State University
The University of Wisconsin

NOTICE

This report was prepared as an account of work sponsored by the United States Government. Neither the United States nor the United States Atomic Energy Commission, nor any of their employees, nor any of their contractors, subcontractors, or their employees, makes any warranty, express or implied, or assumes any legal liability or responsibility for the accuracy, completeness or usefulness of any information, apparatus, product or process disclosed, or represents that its use would not infringe privately-owned rights.

Printed in the United States of America
Available from

National Technical Information Service
U.S. Department of Commerce
5285 Port Royal Road
Springfield, Virginia 22151

Price: Printed Copy \$3.00; Microfiche \$0.95

ARGONNE NATIONAL LABORATORY
9700 South Cass Avenue
Argonne, Illinois 60439

A PROTOTYPE ANALOG REACTIVITY METER
FOR EBR-II

by

J. R. Karvinen, R. W. Hyndman,
R. A. Call, and C. C. Price

EBR-II Project

February 1971

TABLE OF CONTENTS

	<u>Page</u>
ABSTRACT	5
I. INTRODUCTION.	5
II. THEORY.	6
III. MECHANIZATION OF THE KINETIC EQUATIONS	10
A. Delayed-neutron-precursor Circuitry	10
B. Differentiator Development	11
C. Mechanization of the Neutron-population Equation	15
IV. AUTO-RANGING PREAMPLIFIER.	15
V. CALIBRATION AND EVALUATION OF METER	18
A. Calibration.	18
B. Evaluation	19
REFERENCES	24

LIST OF FIGURES

<u>No.</u>	<u>Title</u>	<u>Page</u>
1.	Alternate Methods of Mechanizing the Point-reactor Kinetics Equations	8
2.	Reactivity-meter Diagram	12
3.	Detailed Precursor-loop Circuitry	13
4.	Neutron-signal Differentiator	14
5.	Auto-ranging Preamplifier and Logic Control	16
6.	Response of Precursor Modules to a Square-wave Input	19
7.	Photograph of Reactivity Meter	20
8.	Reactivity-meter Plots for 50- and 500-kW Rod Drops	21
9.	Reactivity-meter Plot for 50-MW Rod-drop Experiment	21
10.	Response of Reactivity Meter to Rod-bump Experiments	22
11.	Response of Reactivity Meter to a Reactor Scram	23

A PROTOTYPE ANALOG REACTIVITY METER FOR EBR-II

by

J. R. Karvinen, R. W. Hyndman,
R. A. Call, and C. C. Price

ABSTRACT

A prototype analog reactivity meter has been developed for EBR-II. Accepting an amplified signal that is proportional to reactor power, the meter uses integrated circuitry to manipulate the incoming signal according to point-kinetic reactor theory and produces a direct readout of reactivity in inhours. This meter, which has been used to monitor all EBR-II operations since July 1969, obtains the first derivative of the neutron flux using a filtered differentiator and incorporates six delayed-neutron groups using closed-loop dynamics. The meter has a frequency response from dc to 40 Hz and can measure reactivity changes with an accuracy of 0.1 Ih (0.03%).

I. INTRODUCTION

A parameter of common interest and usage in reactor operation is "reactivity." However, although reactivity is widely used as a parameter in control of nuclear reactors, it is almost always obtained indirectly from dynamic reactor power. Usually, doing so involves establishing a stable reactor period and relating reactivity to this measured period through the inhour relationship. Although the use of period techniques to determine reactivity are well-proven and widely accepted, direct display of reactivity by a "reactivity meter" can greatly enhance the safety and operation of a nuclear reactor. The advent of fast breeder power reactors with their short neutron lifetimes and fast response times makes use of a reactivity meter with its nearly instantaneous display of reactivity, even more attractive.

The reactivity meter described in this report is an on-line analog instrument that includes electronic simulations of all the terms in the kinetics equations. It can measure small changes in reactivity at varying power levels for long periods. Section II develops the theoretical basis for operation for the meter by using the point-reactor kinetic equations;

Section III discusses mechanization* of these equations. Sections II and III discuss the need for using the first derivative of the concentrations of delayed-neutron precursors and the method of incorporating it into the meter.

The development of a self-ranging preamplifier is discussed in Section IV. Use of this preamplifier allows the reactivity meter to cover four decades of reactor-power variation automatically and effectively removes range problems encountered in earlier meters.^{1,2} Section V evaluates the performance of the meter since it became operational.

II. THEORY

The point-reactor kinetic equations³ are

$$\dot{n}(t) = \frac{(1 - \beta) k(t) - 1}{\ell} n(t) + \sum_{i=1}^N \lambda_i C_i(t) + S(t) \quad (1)$$

and

$$\dot{C}_i(t) = \frac{k(t)\beta_i}{\ell} n(t) - \lambda_i C_i(t), \quad i = 1, N, \quad (2)$$

where

$n(t)$ = time-dependent neutron population of the reactor,

$C_i(t)$ = effective time-dependent population of the i th type of delayed-neutron precursor,

$S(t)$ = effective time-dependent neutron source term,

β_i = effective fraction of delayed neutrons in the i th group,

β = effective delayed-neutron fraction,

λ_i = decay constant of the i th delayed group,

$k(t)$ = instantaneous neutron-multiplication constant,

ℓ = prompt-neutron lifetime of the system,

and

$\dot{n}(t)$ and $\dot{C}(t)$ denote first derivatives with respect to time.

*The arrangement and scaling of electronic circuitry to solve the inverse kinetics equations in analog form.

For a power reactor, the source term $S(t)$ can usually be neglected with an insignificant error, and Eqs. 1 and 2 can be manipulated into the forms

$$\frac{k_{ex}(t)n(t)}{\ell} = \frac{1}{1-\beta} \left[\dot{n}(t) - \sum_{i=1}^N \lambda_i C_i(t) + \frac{\beta}{\ell} n(t) \right], \quad (3)$$

$$\frac{k_{ex}(t)n(t)}{\ell} = \dot{n}(t) + \sum_{i=1}^N \dot{C}_i(t), \quad (4)$$

and

$$\dot{C}_i(t) = \frac{\beta_i}{\ell} [n(t) + k_{ex}(t)n(t)] - \lambda_i C_i(t), \quad (5)$$

where

$$k_{ex}(t) = k(t) - 1$$

and

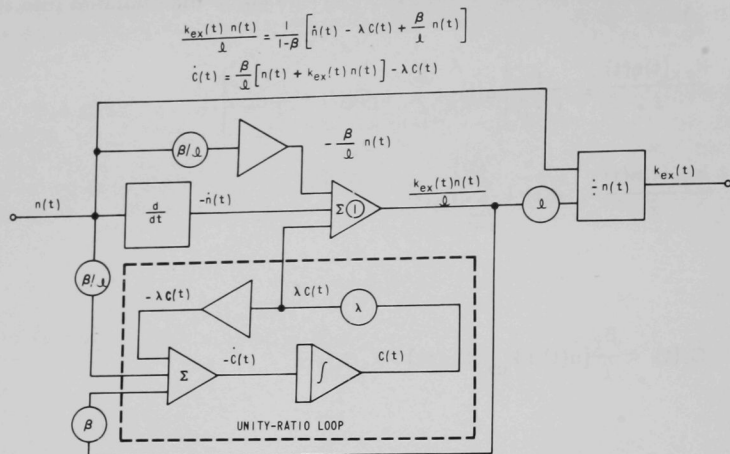
$$k(t) \approx 1.$$

If Eq. 3 is used in the mechanization, an "error" proportional to the reactor power is introduced into the system. The problem results because the circuitry necessary for solution of the $\lambda_i C_i(t)$ terms (i.e., the solution of Eq. 5) contains a minor loop with a unity-ratio system. The equation for the transfer function of these loops is

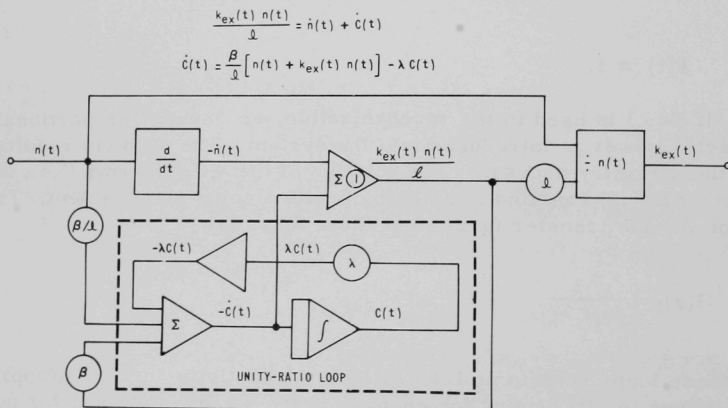
$$G(s)_i = \frac{\lambda_i}{s + \lambda_i}.$$

Since these loops contain no integrations, a reactivity "error" proportional to the change in $n(t)$ occurs for changes in the steady-state reactor power level. Using Eq. 4 in the mechanization avoids the steady-state error caused by the unity-ratio loop by requiring $\dot{C}_i(t)$ rather than $C_i(t)$ as an input for $\frac{k_{ex}(t)n(t)}{\ell}$.

To further clarify the discussion in the previous paragraph, let us consider the problem by using block diagrams of the two mechanization schemes (Fig. 1). To simplify the discussion, assume only one delayed-neutron group. Figure 1a shows a block diagram for mechanization of



a. Unscaled Block Diagram for Mechanization of Eq. 3



b. Unscaled Block Diagram for Mechanization of Eq. 4

Fig. 1. Alternate Methods of Mechanizing the Point-reactor Kinetics Equations

Eq. 3* (one delayed-neutron group). In this case, $\lambda C(t)$ is derived from the unity-ratio minor loop. Figure 1b shows a block diagram for the mechanization of Eq. 4. Here, $\dot{C}(t)$, rather than $\lambda C(t)$, is derived from the minor loop. The characteristic of a unity-ratio system is that when it is changed, the final result is in error by a fraction of the change.⁴ This error is dependent on the loop parameters and the method of the change (i.e., step, ramp, etc.).

Approaching the problem by using heuristic arguments, suppose that at a steady-state reactor power, $n(t) = a$ constant, the meter is scaled and adjusted to indicate $C(t)$, with $k_{ex}(t) = 0$. If the reactor power is raised in a step to $n_1(t)$, then, due to the error in the unity-ratio loop, $C(t)$ moves to $C_1(t) - \epsilon C_1(t)$, where ϵ is the system- and change-dependent error fraction. After the step change, steady-state conditions are established and the output of amplifier 1 (see Fig. 1a) is

$$\frac{k_{ex}(t)n_1(t)}{\ell} = \dot{n}_1(t) - \lambda [C_1(t) - \epsilon C_1(t)] + \frac{\beta}{\ell} n_1(t).$$

For the steady-state conditions,

$$\dot{n}_1(t) = 0,$$

$$\dot{C}_1(t) = 0,$$

and

$$\frac{\beta}{\ell} n_1(t) = C_1(t),$$

from Eqs. 1 and 2. Therefore,

$$\frac{k_{ex}(t)n_1(t)}{\ell} = \epsilon C_1(t).$$

After the computation passes through the "multiply-by- ℓ " potentiometer and "divide-by- $n(t)$ " circuitry,

$$k_{ex}(t) = \epsilon C_1(t),$$

rather than zero as the kinetic equations require. Note that if $\epsilon \rightarrow 0$, then

$$k_{ex}(t) \rightarrow 0.$$

* The $1/(1-\beta)$ multiplier term of Eq. 3 can be neglected with less than 1% error. Errors of this magnitude are less than component tolerances.

When $\dot{C}(t)$ is used (Eq. 4) in the mechanization (Fig. 1b), the unity-ratio error still exists but the output of amplifier 1 is now

$$\frac{k_{\text{ex}}(t)n_1(t)}{\ell} = \dot{n}_1(t) + \dot{C}_1(t) - \epsilon\dot{C}_1(t).$$

For steady-state operation,

$$\dot{n}_1(t) \equiv 0$$

and

$$\dot{C}_1(t) \equiv 0.$$

Since $n_1(t)$ and ℓ are not equal to zero, $k_{\text{ex}}(t) \equiv 0$ at any power level for a critical reactor.

A velocity error exists for Eq. 4, but with the nonlinear term of $n(t)k_{\text{ex}}(t)$ introduced into the total loop, the system does not readily lend itself to a linear analysis. However, the problem can be examined qualitatively. First, $\epsilon C(t)$, the reactivity error is proportional to reactor power, since $C(t)$ is proportional to $n(t)$. The power error then is cumulative, whereas $\epsilon\dot{C}(t)$ is only a function of the rate of change of power and is not cumulative. It is possible to minimize the velocity error for large reactor-power ranges by using special design techniques. This argument may have to be modified for the use of the range-switched preamplifier, but the presence of a steady-state reactivity error in the mechanization of Eq. 3 still makes this mechanization an unacceptable solution.

III. MECHANIZATION OF THE KINETIC EQUATIONS

The reactivity meter was first set up on a Beckman Analog computer to test theory and performance. Results of this experiment provided the impetus to build a prototype instrument. Reactor operating conditions required that the reactivity meter be capable of a reactivity resolution of 0.1 lh over a reactor power range of four decades with $\pm 5\%$ accuracy. To meet these requirements, the delayed-neutron terms are mechanized by using dynamic circuitry, and an automatic ranging preamplifier (described in Section IV) is used to cover the power range.

A. Delayed-neutron-precursor Circuitry

The reactivity meter provides for six delayed-neutron groups. All loops use high-quality, high-gain solid-state amplifiers with low voltage-drift characteristics. These features allow for essentially a one-time calibration for each precursor channel.

Figure 2 shows a diagram of the complete meter system, from ion-chamber input to reactivity output. To facilitate discussion, sections of the diagram appear later in this report as detailed figures.

The following equations determine the necessary values for scaling the precursor equation (Eq. 5) to the electronic circuitry:

$$\frac{\beta}{\ell} n(t) = \frac{R_6}{R_1} n(t), \quad (6)$$

$$10^8 \frac{\beta}{\ell} k_{\text{ex}}(t) n(t) = \frac{R_7}{R_1} k_{\text{ex}}(t) n(t), \quad (7)$$

and

$$-\lambda_i C_i(t) = -\left(\frac{R_4}{R_1}\right) C_i(t). \quad (8)$$

The resistances in the above equations refer to Fig. 3, in which the precursor mechanization is detailed for one precursor. Boxes in Fig. 2 contain the calculated resistance values used to scale the six precursor loops. During calibration of the meter, some adjustment in the calculated values is required to compensate for tolerance variations in the feedback capacitors used in the integrators. To aid in a rapid reset to operational conditions after range switching by the preamplifier, the integration in each precursor loop is equipped with a relay-closed bypass resistor (see Fig. 3).

The data for delayed-neutron precursors used in scaling the reactivity meter are:

Precursor	$\lambda_i, \text{sec}^{-1}$	β_i
1	0.0127	2.584×10^{-4}
2	0.0317	1.514×10^{-3}
3	0.115	1.375×10^{-3}
4	0.311	3.008×10^{-3}
5	1.40	1.047×10^{-3}
6	3.87	2.418×10^{-4}

The value of the prompt-neutron lifetime used in the mechanization is $1.556 \times 10^{-7} \text{ sec.}$

B. Differentiator Development

It is necessary to differentiate the neutron population signal, $n(t)$, to obtain $\dot{n}(t)$ for use in the mechanization of Eq. 4. Since differentiators without a limited bandwidth are inherently unstable, the $n(t)$ differentiator is designed with a pass band that has less than 5% deviation from a flat response from 0 to 40 Hz and then begins to discriminate at higher frequencies.

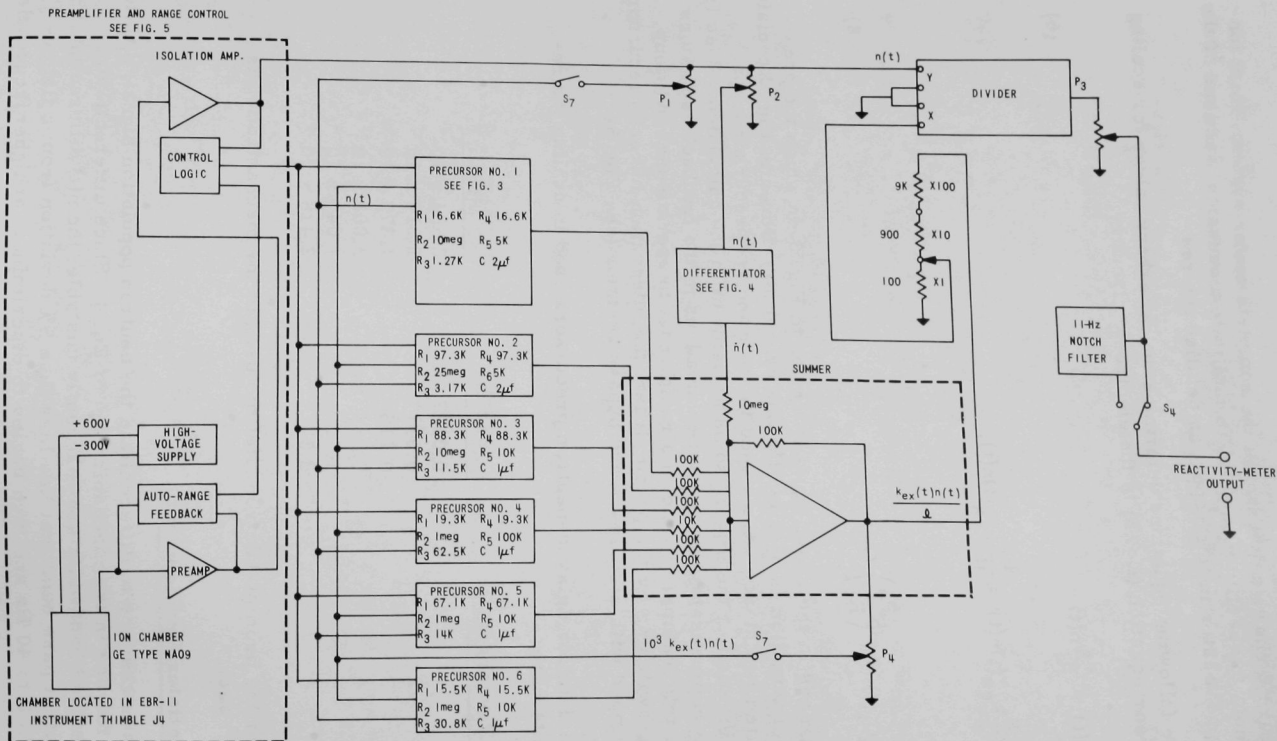
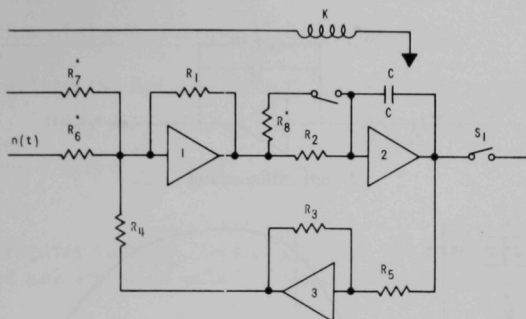


Fig. 2. Reactivity-meter Diagram



*Same resistance values for all precursor loops

R_6 --1K Ω

R_7 --1 meg Ω

R_8 --10K Ω reset resistor

K is relay contact to aid resetting of precursors during range switching

S_1 switch provides a means of dropping an individual precursor group out during calibration and testing

Fig. 3. Detailed Precursor-loop Circuitry

The 40-Hz value was selected on the basis of its 25-msec period, which provides a response approximately 10 times faster than any purposeful movement of rods in the reactor or any credible accident.

Figure 4a shows the differentiator circuit diagram⁶ corresponding to the differentiator block in Fig. 2. From Fig. 4a, the transfer function, $G_d(s)$, of the differentiator is

$$G_d(s) = \frac{R_d C_d s}{(1 + R_d C_f s)^2} \quad (9)$$

Figure 4b shows the Bode plot for Eq. 9.

R_d and C_d are the differentiator resistor and capacitor for the ideal differentiator. R_f is a damping resistor used to prevent oscillations; C_f limits the high-frequency gain.

If the "critical" frequency for the differentiator ω_c is chosen to be 100 Hz, the radian frequency becomes $\omega_c = 100 \times 2\pi$, where $s = j\omega$.

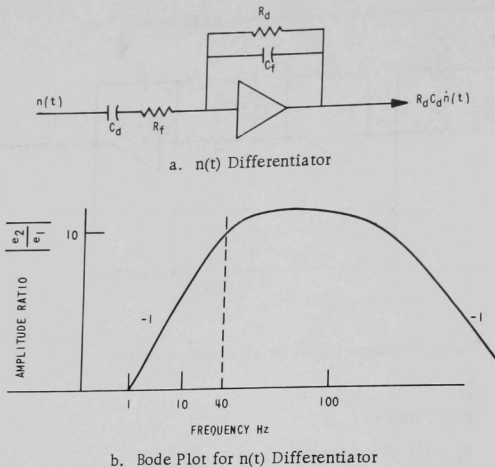


Fig. 4. Neutron-signal Differentiator

For a maximum rate of power increase of 10%/sec, the differentiator component values are

$$\frac{n(t) \max}{\dot{n}(t) \max} = R_d C_d = 10 \text{ sec} = 10^6 \Omega \times 10^{-5} \text{ F}.$$

Now,

$$\omega_c = \frac{1}{R_f C_d} = \frac{1}{R_d C_f}. \quad (10)$$

The values for R_f and C_f are then

$$R_f = \frac{1}{\omega_c C_d} = 160 \Omega$$

and

$$C_f = \frac{1}{\omega_c R_d} = 1600 \text{ pF}.$$

C. Mechanization of the Neutron-population Equation

Having solved the neutron-population equation in the form

$$\frac{k_{\text{ex}}(t)\dot{n}(t)}{\ell} = \dot{n}(t) + \sum_{i=1}^6 \dot{C}_i(t),$$

consider the circuitry in Figs. 1b and 2 again. The time derivatives of the precursor loops are summed with the neutron time derivative, $\dot{n}(t)$, to provide

$$\sum_{i=1}^6 \dot{C}_i(t) + \dot{n}(t)$$

or its equivalent,

$$\frac{k_{\text{ex}}(t)n(t)}{\ell},$$

at the output of the summer amplifier. This signal is fed into a potentiometer, which multiplies the signal by $\ell \times 10^3$. This scaled output, $k_{\text{ex}}(t)n(t) \times 10^3$, is then used as an input to the precursor modules. The output of this amplifier is also taken through another set of scaling resistors to a divider, where it is divided by $n(t)$. Potentiometer P_3 is used to scale the reactivity output of the divider, $k_{\text{ex}}(t)$, to read directly in inhours.

EBR-II has a periodic oscillation in the neutron flux of about 11 Hz.⁵ To remove this frequency component from the reactivity output during steady-state operation when reactivity perturbations have a relatively long time constant, an 11-Hz switchable notch filter is designed into the meter.

IV. AUTO-RANGING PREAMPLIFIER

To cover a reactor operating range of four decades in reactor power, an auto-ranging preamplifier is built into the reactivity meter. This amplifier ranges automatically from 10^{-7} to 10^{-3} A, provides initial conditions for the precursors during each change in range, and has the necessary feedback mechanisms to maintain itself in the proper range.

In the standard preamplifier for ion chambers, large-value resistors are commonly used for feedback. Accuracy of the high resistances is difficult to obtain and even harder to maintain. In this case, a different approach is used to achieve the same results. Figure 5 shows details of the

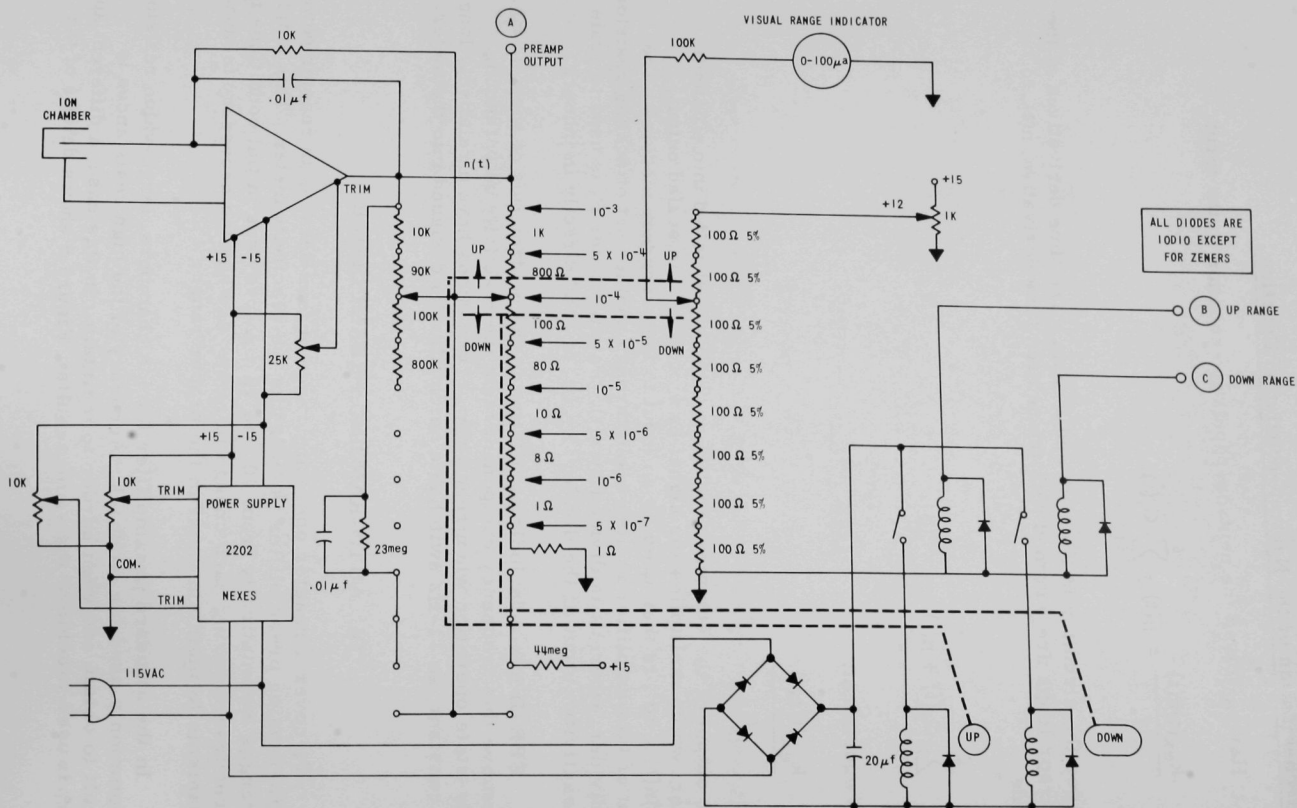


Fig. 5. Auto-ranging Preamplifier and Logic Control

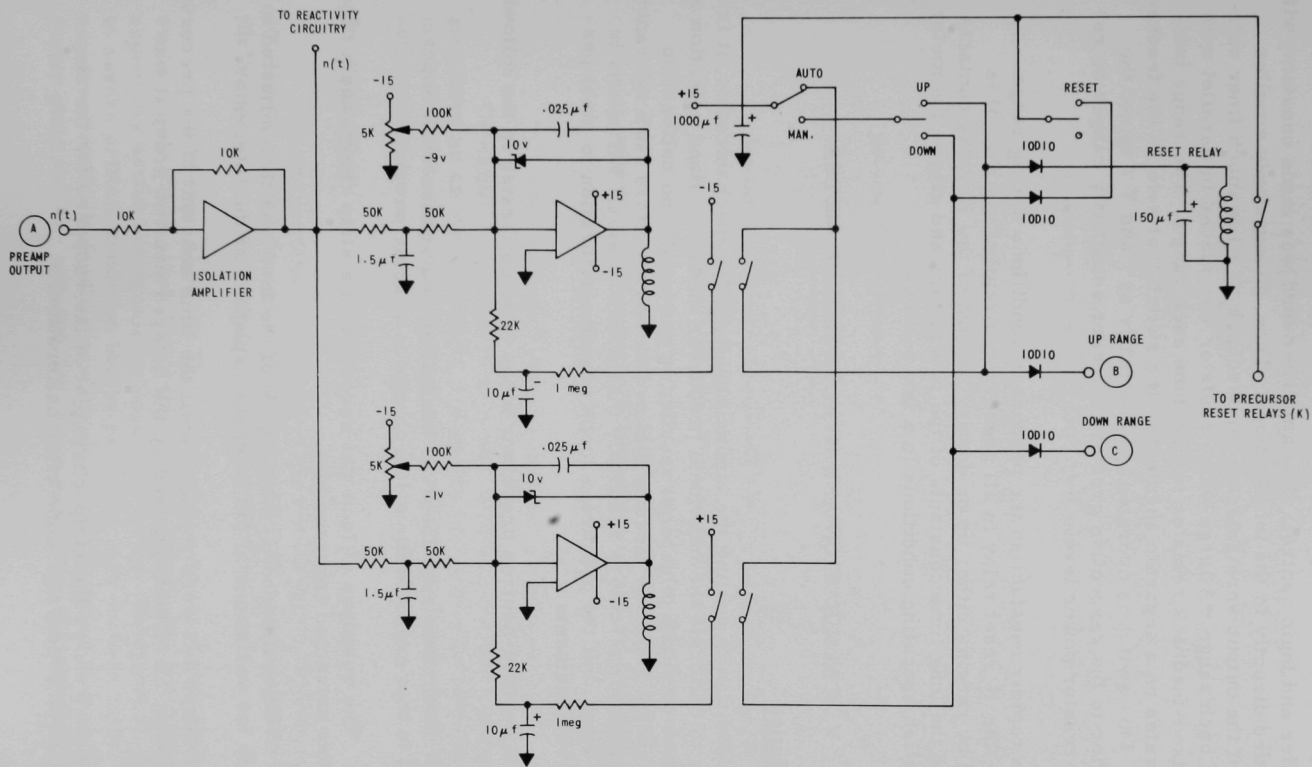


Fig. 5 (Contd.)

preamplifier and logic control. The amplifier load was made constant, with the input tied directly to the ion chamber. Then, successively smaller portions of the output were selected for feedback to allow much finer calibration of each range. A large-value resistor was placed in parallel with a 10-k Ω fixed-feedback resistor to fine-tune each range. The range indicator operates on a separate segment of the switch that selects the feedback resistor. This switch is operated automatically at 1 and 9 V to set the preamplifier to the respective greater or lesser sensitivity ranges as required by reactor power levels.

To rapidly reestablish the precursor conditions during range switching, the K reset relay in all precursor circuits (see Fig. 3) is energized by ranging either up or down. Closure of the K relay contacts eliminates the long time constants of the precursors and allows the meter to reestablish operating conditions in a few seconds.

V. CALIBRATION AND EVALUATION OF METER

A. Calibration

In addition to scaling the kinetic equations for mechanization, it is necessary to calibrate the individual precursor modules. Hand selection of the resistors used (1% tolerance) resulted in essentially no calibration problem, except for those circuits that contained capacitors (10% tolerance). The differentiator circuit is relatively insensitive to small variations in capacitor value, but the precursor loops require calibration to meet performance requirements.

The delayed-neutron precursor loops were calibrated in the following manner:

1. Each precursor loop was energized by a square-wave input equivalent to that expected for a 10% change in reactor power.
2. The response of loop was recorded on a strip chart, and a time constant was extracted from the plot.
3. The resistance R_2 (see Fig. 3) of the loop was then adjusted to compensate for variations in the feedback capacitor of the integrator.
4. Steps 1-3 were repeated until the time constant of the precursor loop was within 3% of that required by the delayed-neutron group it was simulating.

Figure 6 shows the strip-chart plot of the response for the six delayed-neutron precursor loops after calibration.

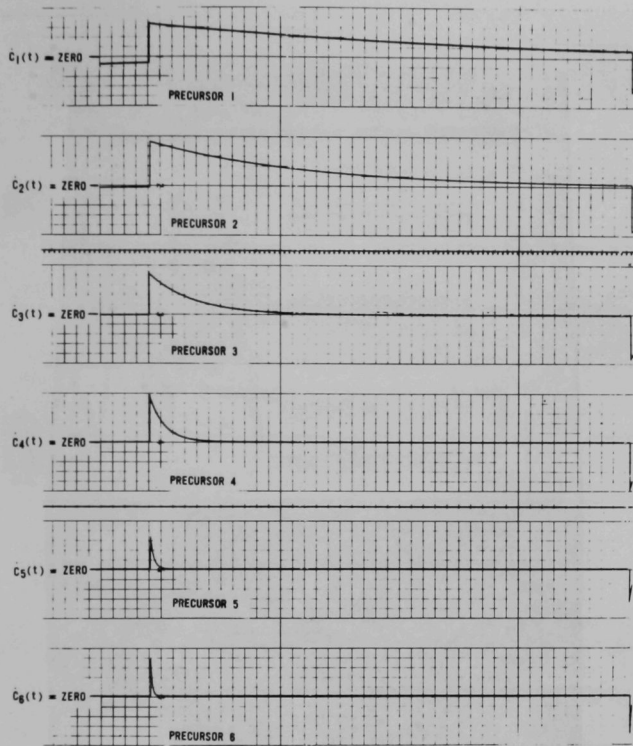


Fig. 6. Response of the Precursor Modules to a Square-wave Input

To calibrate the meter as a unit, a 10% step change in power was simulated as an input for $n(t)$. The meter was then calibrated to 30.3 Ih for a 10% step change in reactor power using the prompt-jump kinetics approximation.

B. Evaluation

The preamplifier response of the reactivity meter was reduced to 500 Hz (-3 dB) to eliminate high-frequency spikes that might be caused in the signal by the automatic-ranging mechanism.

The meter, shown in Fig. 7, has been used to monitor all EBR-II reactor operations since July 1969. In this period, the meter has been especially useful in monitoring reactivity during experiments. It is used to assure critical condition before rod-drop experiments and to verify that negative reactivity feedback exists at power. Figure 8 shows the reactivity-meter plots for 50- and 500-kW (zero-power) rod drops in EBR-II for

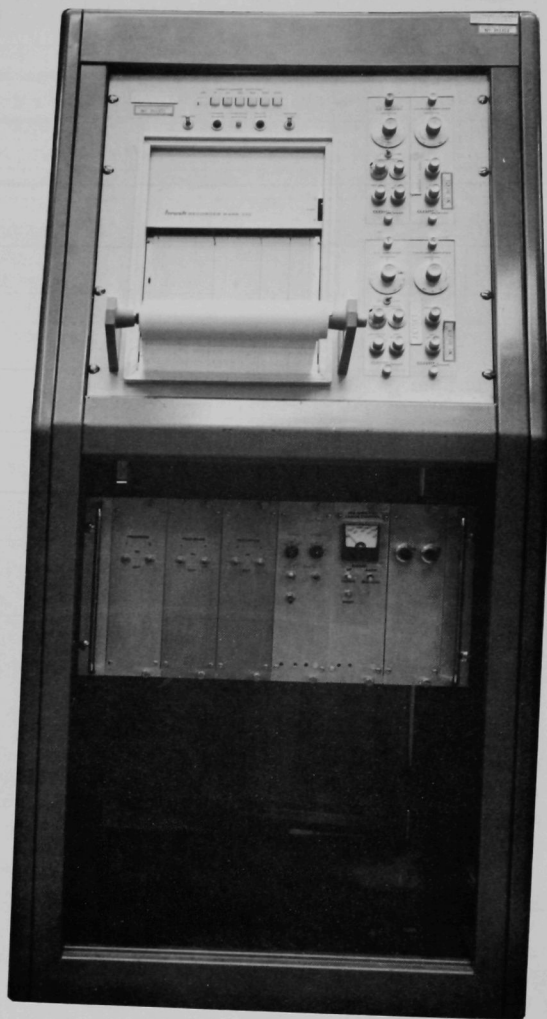


Fig. 7. Photograph of Reactivity Meter

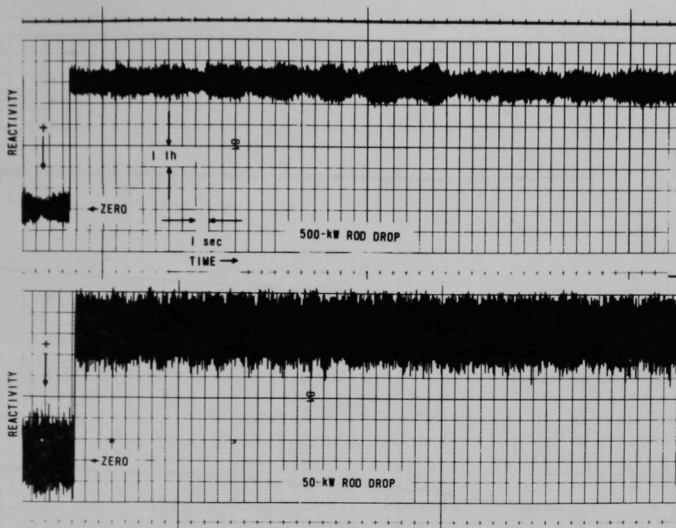


Fig. 8. Reactivity-meter Plots for 50- and 500-kW Rod Drops

reactor run 41A. Figure 9 shows the neutron signal and the reactivity for EBR-II rod-drop experiments at power (50 MWt). Clearly evident in this figure is the negative reactivity feedback. Figure 10 shows recent results of "rod-bump" experiments monitored by the meter. The noise in the data is due, in large part, to the low efficiency of the ion chamber, which is a considerable distance from the reactor core, and to a lesser extent on extraneous noise, such as 60 Hz.

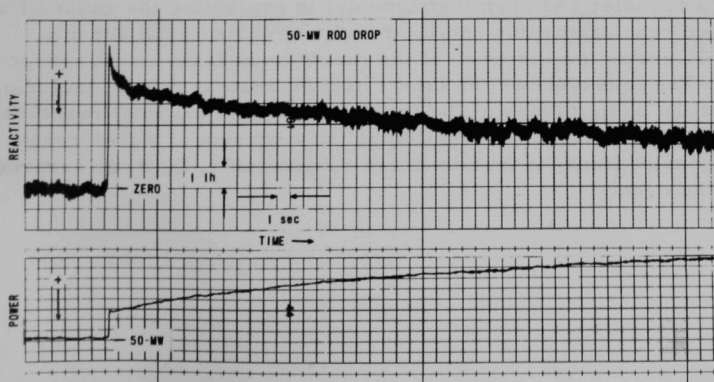


Fig. 9. Reactivity-meter Plot for 50-MW Rod-drop Experiment

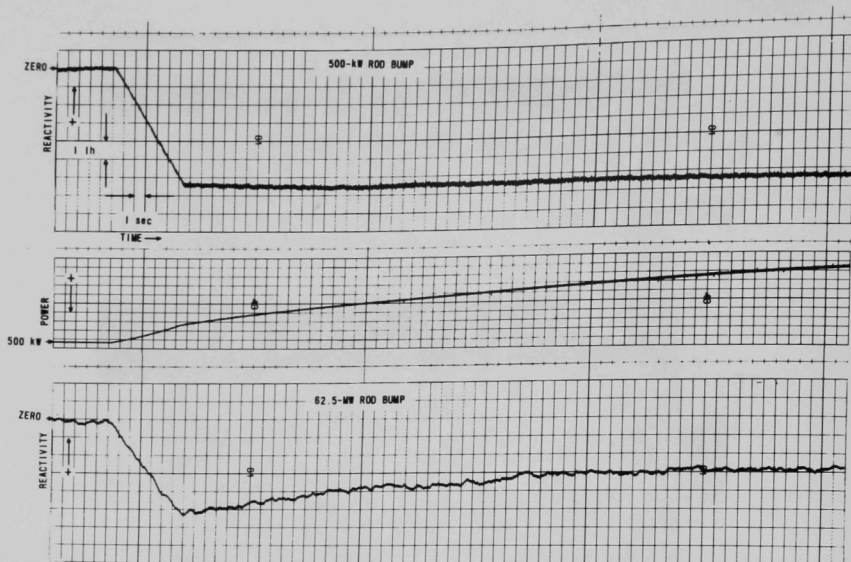


Fig. 10. Response of Reactivity Meter to Rod-bump Experiments

At zero power, the reactivity meter shows agreement within 4% for control-rod worths when compared with values obtained by control-rod calibrations in which period measurements were used. Additional testing has shown the meter to be readily capable of measuring reactivity changes on 0.1 Ih ($\approx 0.03\%$); the main limitation on this accuracy is the noise on the input neutron-population signal.

The meter has been instrumental in explaining the cause of unscheduled reactor scrams and the reactivity during such scrams. Figure 11 shows the response of the meter to an inadvertent overpower scram. The figure shows the total effect on reactor power, including the effect of the auto-ranging of the preamplifier, and the total reactivity inserted. Also included in this plot is the response of a fuel-center thermocouple, from the instrumented subassembly, that was recorded during the event.

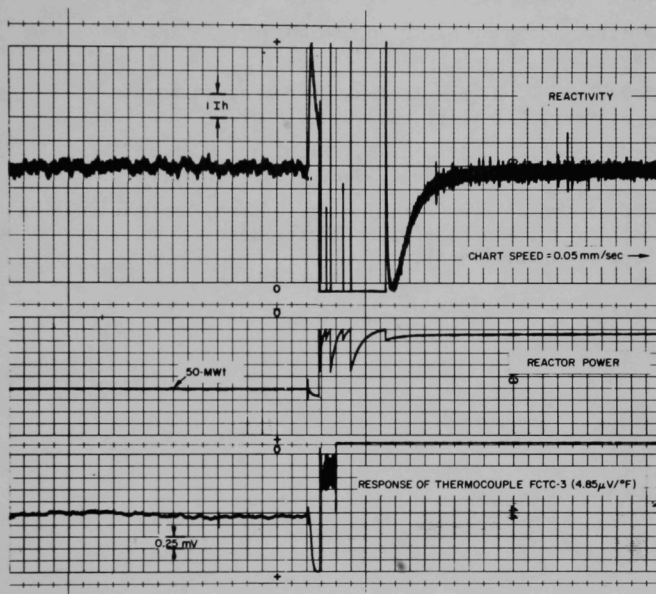


Fig. 11. Response of Reactivity Meter to a Reactor Scram

REFERENCES

1. H. Atkinson, P. R. James, and D. Tait, *Design and Use of Simple Reactivity Meters for Fast Reactors*, United Kingdom Atomic Energy Authority, TRG Report 1526(D) (1967).
2. H. Walze, *Construction and Performance of SNEAK Reactivity Meter*, EURATOM Fast Reactor Exchange EURFNR 519, Report KFK 739 (Mar 1968).
3. R. O. Brittan, *Some Problems in the Safety of Fast Reactors*, ANL-5577, p. 6 (May 1956).
4. J. L. Bower and P. M. Schulteiss, *Introduction to the Design of Servomechanisms*, Wiley, pp. 233-242 (1958).
5. R. W. Hyndman, F. S. Kirn, R. R. Smith, and H. Kuroi, *EBR-II Self-excited Oscillations*, Trans. Am. Nucl. Soc. 8(2), 590 (1965).
6. *Applications Manual for Computing Amplifiers for Modeling Measuring Manipulating and Much Else*, Philbrick Researches, Inc., Nimrod Press, Inc., Boston, Mass. (1966).

